Diffuse γ-ray emission from a synthetic Galactic population of young stellar clusters

S. Menchiari,[a,*] G. Morlino,[a] E. Amato[a] and N. Bucciantini[a]

[a]*INAF - Osservatorio Astrofisico di Arcetri,*
Largo Enrico Fermi 5, Firenze, Italy

E-mail: stefano.menchiari@inaf.it, giovanni.morlino@inaf.it

In recent years, several young massive star clusters (YMSCs) have been associated with extended γ-ray sources, suggesting that some acceleration process, able to accelerate particles at least up to hundreds of TeV, is at work. The number of YMSCs with associated γ-ray emission is of order ten, however the number of potential sources is much larger, probably up to several hundreds. It is plausible that many such objects have not been observed yet due to their low surface brightness. However, such unresolved sources may contribute to the diffuse Galactic γ-ray background. In this work, we aim at estimating the total contribution of unresolved YMSCs to the diffuse γ-ray flux. This is done based on a synthetic population built from observed properties of local (within 2 kpc from the Sun) clusters. We simulate the Galactic population of YMSCs using a Montecarlo approach. For each cluster, we build the stellar population, in order to estimate the collective wind luminosity and mass loss rate. The γ-ray emission of each cluster is then computed assuming a pure hadronic scenario, where protons are accelerated at the collective wind termination shock of the stellar cluster and subsequently interact with the material embedded inside the wind-blown bubble. We also consider different scenarios of particle transport inside the bubble, an important ingredient that determines both the maximum energy and the escape time from the bubble, thus affecting the final γ-ray spectrum. Our results are then compared with measurements of the diffuse γ-ray flux provided by several experiments, from a few GeV to hundreds of TeV.

---

*Speaker

1. Introduction

Stellar clusters are among the most studied celestial objects in the Cosmos and represent the fundamental building blocks of galaxies. In the last decades, several experiments have detected diffuse γ-ray emission in coincidence with a dozen Galactic young (<10 Myr) massive (>10^3 $M_\odot$) star clusters (YMSCs), among which Cygnus OB2 [1, 6, 7], Westerlund 1 [2, 4], and Westerlund 2 [29]. The detection of γ-ray emission can be easily explained if $\sim 10\%$ of the power supplied by the strong winds from the massive stars hosted by the clusters is used to accelerate cosmic rays (CRs) [3].

During the years, several mechanisms of particles acceleration have been proposed [11, 19, 26, 27]. In the case of young compact clusters, the winds of the massive stars may combine to generate a collective cluster wind. In this scenario, particle acceleration is expected at the collective cluster wind termination shock (TS) [23]. After acceleration, CRs escape from the TS and start to propagate within the bubble created by the expanding hot shocked wind material. Here, the diffusion is suppressed due to the highly turbulent nature of the hot shocked plasma. As a result, the bulk of the accelerated particles remain confined within the bubble itself. In a pure hadronic scenario, this produces γ-ray emission with a size comparable to that of the wind blown bubble, which is consistent with the observed sizes ($\sim 1° - 3°$) of the γ-ray radiation detected in coincidence with stellar clusters.

In general, detecting diffuse emissions in γ-ray astronomy is challenging due to the problematic background subtraction. Consequently, the detection of YMSCs in γ-ray can suffer from observational biases. At present, it is reasonable to expect that most of the emission coming from YMSCs is indirectly observed as a contribution to the large-scale Galactic emission. In this work, we aim to estimate such a contribution by generating a synthetic galactic population of YMSCs based on known properties of observed local clusters. For each cluster, we simulate a mock population of stars whence the parameters of the collective cluster wind are estimated. We compute the CR content in each cluster using the model provided by [23], and we then calculate the associated γ-ray emission assuming a pure hadronic nature.

The paper is structured as follows: In §2, we describe the method for the simulation of the mock star population in each cluster, and the recipes used to model the stellar wind physics. In §3, we illustrate the approach employed for the simulation of the synthetic YMSC population. In §4, we summarize the model of CR acceleration at the wind TS developed by [23] and the procedure used to compute the γ-ray emission. In §5, we compare the diffuse emission from the Galactic population with available data in the literature, and we then discuss the obtained results. Finally, we present in §6 the conclusion of the work.

2. Generation of a stellar population inside YMSCs and estimation of the cluster wind parameters.

For every YMSC, the mock stellar population is built starting from two fundamental parameters: the cluster age and mass. The process can be summarized in two main steps: first, starting from the cluster mass, we extract a population of stars by random sampling the initial stellar mass function (IMF). Afterward, based on the cluster age, we remove all the stars that are expected to have

exploded as supernovae. In the first step, when sampling the IMF, we consider that the number of stars in a given cluster is:

$$N_\star(M_{SC}) = M_{SC} \frac{\int_{M_{\star,min}}^{M_{\star,max}} f_\star(M_\star) dM_\star}{\int_{M_{\star,min}}^{M_{\star,max}} M_\star f_\star(M_\star) dM_\star} \tag{1}$$

where all quantities with the subscript $\star$ refers to stellar parameters. M_{SC} is the mass of the star cluster and $f_\star(M_\star)$ is the stellar IMF [20]. The minimum and maximum stellar masses that can be generated within a cluster are $M_{\star,min} = 0.08$ M$_\odot$, which is related to the minimum theoretical mass to support significant nuclear burning [13], and $M_{\star,max} = 150$ M$_\odot$ that is the maximum observed stellar mass in clusters [32]. In the second step, we remove all those stars that exploded as supernova by considering that a star with a given mass $M_\star$ will leave the main sequence (and soon after explode as a supernova) at a turn-off time (t_{TO}) given by the following relation [10]:

$$\log\left(\frac{t_{TO}}{1 \text{ yr}}\right) = 0.825 \log^2\left(\frac{M_\star}{120 \text{ M}_\odot}\right) + 6.43 . \tag{2}$$

All the stars with a turn-off time less than the cluster age are removed from the cluster.

2.1 Modeling stellar winds

We model the physics of stellar winds using a purely empirical approach. The mass loss rate ($\dot{M}_\star$) for a given star is calculated using the relation provided by [24]:

$$\log\left(\frac{\dot{M}_\star}{\text{M}_\odot \text{yr}^{-1}}\right) = -14.02 + 1.24 \log\left(\frac{L_\star}{\text{L}_\odot}\right) + 0.16 \log\left(\frac{M_\star}{\text{M}_\odot}\right) + 0.81\left(\frac{R_\star}{\text{R}_\odot}\right) . \tag{3}$$

The kinetic luminosity of the stellar winds is defined as:

$$L_{\star,w} = \frac{1}{2}\dot{M}_\star \left\{ C(T_{\text{eff}})^2 \left[\frac{2GM_\star(1 - L_\star/L_{\text{Edd}})}{R_\star} \right] \right\} \tag{4}$$

where the term in braces represents the wind speed squared [21], and L_{Edd} is the Eddinghton luminosity. The coefficient $C(T_{\text{eff}})$ depends on the stellar temperature and is obtained from observations [21]. Both the mass loss rate and the wind luminosity depend on stellar parameters, such as stellar luminosity ($L_\star$), stellar radius ($R_\star$), and effective temperature (T_{eff}). We again rely on a purely empirical approach to estimate the stellar luminosity and radius. As we are considering stars over a large range of masses, the empirical method is preferred to stellar models as the latter are often defined on narrow mass intervals.

For what concerns the stellar luminosity, we consider the mass-luminosity relation presented in [22] (Eq. 3.7). This consists of a smoothed broken power law mixing two different empirical mass-luminosity relations: the first one provided by [15] and valid between 0.179–31 M$_\odot$, and the second one provided by [30] valid for very massive stars ($M_\star > 100$ M$_\odot$). To estimate stellar radius, we use the mass-radius relation presented in [14]: $R_\star = 0.85 \left(\frac{M_\star}{M_\odot}\right)^{0.67}$ R$_\odot$. Finally, we calculate the effective stellar temperature using the Boltzmann law: $T_{\text{eff}} = \left[\frac{L_\star}{4\pi R_\star^2 \sigma_b}\right]^{1/4}$, where σ_b is the

3

Boltzmann constant.

Once the wind luminosity and mass loss rate of every star are known, the collective cluster wind luminosity (L_w) and mass loss rate ($\dot{M}$) are straightforwardly calculated as $L_w = \sum_i L_{\star,w,i}$ and $\dot{M} = \sum_i \dot{M}_{\star,i}$ respectively.

3. Generating synthetic population of Galactic YMSCs

The core ingredient used to simulate the Galactic YMSCs is the cluster distribution function: $\xi_{SC}(M, t, r, \theta) = \frac{dN_{SC}}{dM_{SC}dtdrd\theta}$, defined such that the total number of clusters in the Milky Way with masses ranging in a given interval $[M_{min}, M_{max}]$, and age $[t_{min}, t_{max}]$ is

$$N_{SC} = \int_{M_{min}}^{M_{max}} \int_{t_{min}}^{t_{max}} \int_0^{R_{MW}} r\xi_{SC}(M_{SC}, t, r)dM_{SC}dtdrd\theta \,, \tag{5}$$

where R_{MW} is the Milky Way radius. As we are interested in young and massive stellar clusters, we consider $t_{min} = 0$, $t_{max} = 10$ Myr and $M_{min} = 10^3$ M$_\odot$. The maximum cluster mass is derived from observations [25], and is $M_{max} = 6.3 \times 10^4$ M$_\odot$. The true form of ξ_{SC} is not known. However, a reasonable assumption is that the distribution can be factorized in mass, time, and space, so that ξ_{SC} can be written as $\xi_{SC}(M, t, r) = f(M_{SC})\psi(t)\rho(r, \theta)$, where $f(M_{SC})$, $\psi(t)$, and $\rho(r, \theta)$ are the cluster initial mass function, the cluster formation rate and the cluster spatial distribution respectively.

It is possible to infer both the cluster formation rate and cluster mass function from observations. In this regard, we consider the work carried out by [25], based on a local survey of stellar clusters (Milky Way Star Cluster Survey). In [25] the cluster initial mass function is modeled as a broken power law. For clusters with $M_{SC} > 10^3$ M$_\odot$, the cluster mass function is $f(M_{SC}) = 1.2M_{SC}^{-1.54}$. After correcting for the effect of cluster evolution, the age distribution of stellar clusters is found to be flat in the last tens of Myrs [25]. This implies a constant cluster formation rate in the last 10 Myr, so that $\psi(t) = \bar{\psi} = const$. We calculate the cluster formation rate using the observed star formation rate inferred from embedded young stellar clusters as measured by [9], which leads to an average cluster formation rate of $\bar{\psi} = 1.8$ Myr^{-1} kpc^{-2} [22].

We model the YMSCs spatial distribution in the Milky Way following the approach presented in [22]. The method can be summarized into two main steps: first, the galactocentric radial position and the altitude of stellar clusters are extracted. The galactocentric position is obtained assuming that young cluster follow the same radial distribution of giant molecular clouds, which is inferred from the catalog provided by [16]. The altitude position is instead extracted assuming that clusters follow the same exponential distribution of the observed gas profile. Secondly, based on their radial and angular position, YMSCs are associated with a specific Galactic structure, i. e. spiral arm, galactic bar, etc. To this end, we model the Milky Way structure following the work by [16]. The criteria for the association of each Galactic structure are summarized in [22] (Tab. 3.1).

Inserting all the aforementioned distributions in Eq. 5, we find a total of 747 YMSCs. We find an average value for the wind luminosity and mass loss rate of $\overline{L_w} \approx 3 \times 10^{36}$ erg s^{-1} and $\overline{\dot{M}} \approx 10^{-6}$ M$_\odot$ yr^{-1} respectively.

4. Cosmic ray acceleration at the collective wind termination shock of YMSCs

When the average distance between stars in a cluster is less than the single stellar winds termination shocks (TS), the winds from the massive stars combine to create a collective cluster wind. This scenario is typical of young clusters as a direct consequence of primordial mass segregation (see [22] and references therein). As the wind material gets shocked and heated, it adiabatically expands in the interstellar medium (ISM) generating large bubble-like structures similar to those observed close to single massive stars [28]. A model for particle acceleration in these systems was presented in [23]. The model can be summarized as follow: particles are accelerated at the collective cluster wind TS via the diffusive shock acceleration mechanism, and subsequently escape from the acceleration site experiencing a combination of advection and diffusion in the hot bubble until the border of the bubble is reached. From there, CRs are free to escape in the unperturbed ISM.

Given the highly turbulent nature of the hot bubble, particle diffusion is suppressed. As a result, most of the injected CRs remain confined within the bubble borders, and the majority of the γ-ray emission is produced in this region. The CR distribution in the bubble is [23]:

$$f(r, p) = f_{TS}(p)\mathcal{G}(D_2, R_b) , \tag{6}$$

where

$$f_{TS}(p) = \mathcal{A}(\epsilon_{CR}, L_w, \dot{M}) \left(\frac{p}{m_p c}\right)^{-4} \left[1 + a_1 \left(\frac{p}{p_{max}}\right)^{a_2}\right] e^{-a_3 (p/p_{max})^{a_4}} . \tag{7}$$

The parameters a_1, a_2, a_3 and a_4 depend on the spectral behavior of the diffusion coefficient, which is ultimately related to the type of magnetohydrodynamic turbulence spectrum. In this work, we will consider two different scenarios of a Kraichnan spectrum and a Bohm-like diffusion. The coefficients are listed in [22] (Tab. 1.1). The parameter $\mathcal{A}$ is a normalization factor which depends on the cluster wind power, mass loss rate and the efficiency of CR production ($\epsilon_{CR} = 0.1$) (see [22], Eq. 1.75). The function $\mathcal{G}$ (see [22], Eq. 1.70b and Eqs. 1.71) depends on the diffusion coefficient in the bubble (D_2) and the size of the bubble, which is [28]: $R_b = 0.798 L_w^{1/5} \rho_0^{-1/5} t^{3/5}$, where t is the age of the YMSC, and ρ_0 is the average density close to the YMSC that we assume to be $10 m_p$ cm^{-3} (m_p is the mass of the proton). When calculating the diffusion coefficient in the system, we assume for the Kraichnan case that the turbulence is injected at a characteristic length scale of 1 pc. The parameter p_{max} is the maximum momentum reachable by particle acceleration, which can be found by the condition $D_1(p_{max})/v_w = R_{TS}$, where D_1 is the diffusion coefficient in the cold cluster wind, $v_w = (2L_w/\dot{M})^{1/2}$ is the collective cluster wind speed and $R_{TS} = 0.791 \dot{M}^{1/2} v_w^{1/2} L_w^{-1/5} \rho_0^{-3/10} t^{2/5}$ is the size of the TS [28].

The γ-ray flux from a single YMSC is calculated as follows:

$$\phi_\gamma(E_\gamma) = \frac{cn_0}{d^2} \int \int_{R_{TS}}^{R_b} r^2 f(r, E_p) \frac{d\sigma(E_p, E_\gamma)}{dE_p} dr dE_p \tag{8}$$

where $d\sigma/dE_p$ is the differential cross section for γ-ray production through hadronic interaction [18], d is the distance from from the Earth of the YMSC and n_0 is the target density. We here assume two possible values for the target density: $n_0 = 10$ cm^{-3} and $n_0 = 1$ cm^{-3}. Both densities

are likely overestimated and the obtained γ-ray flux has to be interpreted as an upper limit on the emission [22].

5. Comparison of the diffuse γ-ray radiation from YMSCs with observations

Based on the information available in five different works in the literature, we select two regions from which we extract the γ-ray emission from the population of YMSCs. In the first region (named ROI1), spanning between $100° < l < 25°$ and $-5° < b < 5°$, the measurement of the γ-ray flux is provided by [17], [8], and [5], based on observations of EGRET, ARGO, and Tibet-ASγ respectively. The emission in the second region (named ROI2), defined between $125° < l < 15°$ and $-5° < b < 5°$, is provided by [12] and [31], based on LHAASO and Fermi-LAT observations.

We calculate the diffuse γ-ray emission from ROI1 by simply summing up all the fluxes of the YMSCs whose position falls within the region boundaries. For ROI2, we use a different approach. After calculating the emission of γ-rays for each YMSC, we assume that the entire flux is uniformly emitted within a disc equivalent to the size of the projected wind bubble. Subsequently, we determine the diffuse emission in the area by applying the same masks employed to extract the LHAASO and Fermi-LAT data [12, 31].

Fig. 1 shows the diffuse γ-ray spectrum in ROI1. The emission at low-energy ($E_γ < 10$ GeV), in all cases under analysis, is an order of magnitude below the observed flux. On the contrary, for $E_γ \gtrsim 300$ GeV the flux for the Bohm case is found to be larger than what measured by ARGO by a few tens of percent between 0.2 TeV $\lesssim E_γ \lesssim 1$ TeV and a factor ~ 3 at $E_γ \approx 1 - 2$ TeV. For the Kraichnan case, the flux is instead below the observed flux by a factor of ~ 2 at 0.2 TeV $\lesssim E_γ \lesssim 1$ TeV, while at $E_γ \approx 1 - 2$ TeV the expected flux matches the observations. This is indeed an intriguing result, indicating that the non-resolved diffuse emission from YMSCs between a few hundreds of GeV and a few TeV is likely not negligible and possibly even dominant. Even with a target density of 1 cm^{-3}, the diffuse emission at 1 TeV in the Bohm case remains non negligible. Above 100 TeV the emission is only important in the Bohm case, and in the case of very high target density. When considering 1 cm^{-3}, the flux is a factor of a few below the observed data points.

Fig. 2 shows the diffuse γ-ray spectrum in ROI2. Similarly to ROI1, we found the flux at low energy (< 10 GeV) to be negligible. The diffuse emission from YMSCs starts to be important above a few TeVs, consistently with the result in ROI1. We also found the emission in the Bohm scenario to be relevant in the LHAASO range, also if the considered particle density is 1 cm^{-3}. However, due to the small area used to extract the γ-ray emission, the spectrum in this energy range is affected by the statistical fluctuation of the number of stellar clusters with $M_{SC} > 10^4$ M$_\odot$. In order to obtain a robust estimate on the contribution in this energy range, an average flux value obtained from multiple simulations of the Galactic population is required.

In addition to the comparison of the overall emission with γ-ray data, we also investigate the relative contribution to the diffuse γ-ray emission as a function of the cluster mass. We found that the emission is dominated by the most massive stellar clusters. This can be also crosschecked by calculating the differentiated γ-ray luminosity as a function to of cluster mass:

$$\frac{dL_γ}{dM_{SC}} = L_γ(M_{SC})f(M_{SC}) \propto M_{SC}^{-0.5}n_0 t .\tag{9}$$
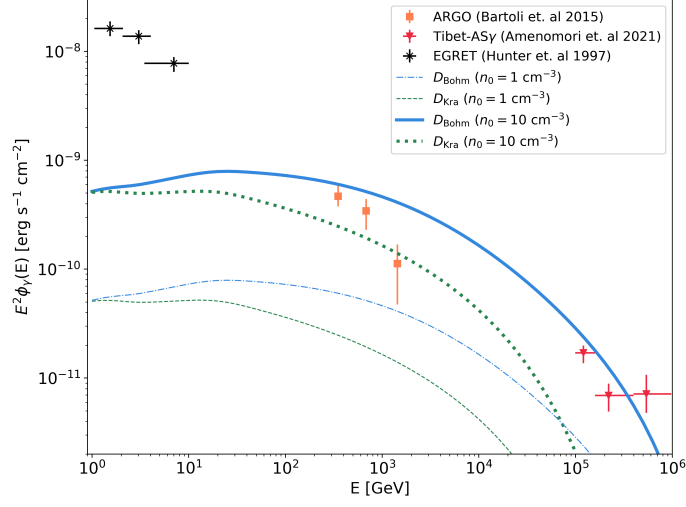
Figure 1: Diffuse γ-ray emission from the synthetic population of YMSCs compared to EGRET, ARGO and Tibet-ASγ observations in ROI1. Thin and thick lines represent the spectra after considering a target density of 10 cm^{-3} and 1 cm^{-3} respectively. Solid and dot-dashed (light blue) lines are the spectra obtained in the case of Bohm-like turbulence. Dotted and dashed (green) lines are instead the spectra calculated for Kraichnan diffusion.
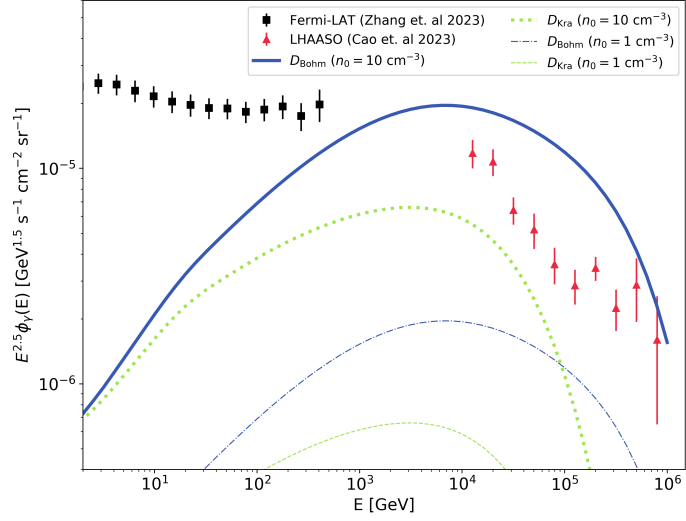

Figure 2: Same as Fig. 1, but for the sky region ROI2.

where t is the cluster age. For a given mass interval of cluster masses between $M_{min,SC}$ and $M_{max,SC}$, the γ-ray luminosity is:

$$L_\gamma \propto \int_{M_{min,SC}}^{M_{max,SC}} M_{SC}^{-0.5} \propto M_{max,SC}^{0.5} \, , \tag{10}$$

if $M_{min,SC} \ll M_{max,SC}$.

7

6. Conclusions

The advancement of highly sensitive γ-ray telescopes in recent decades has led to the identification of several massive star clusters as significant sources of γ-ray emission. This discovery has revealed their role as galactic CR accelerators. Detecting these objects is challenging due to their characteristic diffuse emission, and a substantial portion of their emitted γ-ray flux is likely observed as a contribution to the diffuse emission observed along the Galactic plane. In this work, we estimated this contribution by simulating a synthetic galactic population of YMSCs, starting from observed properties of local clusters. We model the emission from each synthetic YMSC considering a pure hadronic scenario and assuming that particle acceleration is achieved at the collective cluster wind termination shock. We found the diffuse γ-ray emission from the cluster population in two regions of the Galactic plane to be nonnegligible at a few TeV. The contribution is particularly relevant if a Bohm-like diffusion coefficient mediates the particle propagation in the bubble generated by the cluster wind. If diffusion is generated by Kraichnan-like turbulence, the γ-ray emission is relevant only if the target density is relatively high.

References

[1] Abeysekara A. U., et al., 2021, Nature Astronomy, 5, 465

[2] Abramowski A., et al., 2012, , 537, A114

[3] Aharonian F., Yang R., de Oña Wilhelmi E., 2019, Nature Astronomy, 3, 561

[4] Aharonian F., et al., 2022, arXiv e-prints, p. arXiv:2207.10921

[5] Amenomori M., et al., 2021, , 126, 141101

[6] Astiasarain X., Tibaldo. L., Martin P., Knödlseder J., Remy Q., 2023, arXiv e-prints, p. arXiv:2301.04504

[7] Bartoli B., et al., 2014, , 790, 152

[8] Bartoli B., et al., 2015, , 806, 20

[9] Bonatto C., Bica E., 2011, , 415, 2827

[10] Buzzoni A., 2002, , 123, 1188

[11] Bykov A. M., Marcowith A., Amato E., Kalyashova M. E., Kruijssen J. M. D., Waxman E., 2020, , 216, 42

[12] Cao Z., et al., 2023, arXiv e-prints, p. arXiv:2305.05372

[13] Carroll B. W., Ostlie D. A., 1996, An Introduction to Modern Astrophysics

[14] Demircan O., Kahraman G., 1991, , 181, 313

[15] Eker Z., et al., 2018, , 479, 5491

[16] Hou L. G., Han J. L., 2014, , 569, A125

[17] Hunter S. D., et al., 1997, , 481, 205

[18] Kafexhiu E., Aharonian F., Taylor A. M., Vila G. S., 2014, Physical Review D, 90, 123014

[19] Klepach E. G., Ptuskin V. S., Zirakashvili V. N., 2000, Astroparticle Physics, 13, 161

[20] Kroupa P., 2001, , 322, 231

[21] Kudritzki R.-P., Puls J., 2000, , 38, 613

[22] Menchiari S., 2023, arXiv e-prints, p. arXiv:2307.03477

[23] Morlino G., Blasi P., Peretti E., Cristofari P., 2021, , 504, 6096

[24] Nieuwenhuijzen H., de Jager C., 1990, , 231, 134

[25] Piskunov A. E., Just A., Kharchenko N. V., Berczik P., Scholz R. D., Reffert S., Yen S. X., 2018, , 614, A22

[26] Reimer A., Pohl M., Reimer O., 2006, The Astrophysical Journal, 644, 1118

[27] Vieu T., Gabici S., Tatischeff V., Ravikularaman S., 2022, , 512, 1275

[28] Weaver R., McCray R., Castor J., Shapiro P., Moore R., 1977, , 218, 377

[29] Yang R.-z., de Oña Wilhelmi E., Aharonian F., 2018, , 611, A77

[30] Yungelson L. R., van den Heuvel E. P. J., Vink J. S., Portegies Zwart S. F., de Koter A., 2008, , 477, 223

[31] Zhang R., Huang X., Xu Z.-H., Zhao S., Yuan Q., 2023, arXiv e-prints, p. arXiv:2305.06948

[32] Zinnecker H., Yorke H. W., 2007, , 45, 481